

# Experimental Confirmation of the Dynamics of Coupled-Oscillator Arrays and Implications for Angle-Based Modulation

Ronald J. Pogorzelski, *Fellow, IEEE*

**Abstract**—This paper describes a set of experimental measurements designed to test the predictions of the continuum theoretical model concerning the dynamics of a linear array of mutually injection-locked voltage-controlled oscillators. The model indicates that the phase distribution evolves according to a diffusion process, the diffusion rate being determined by the inter-oscillator locking range. The theoretical predictions are confirmed by the experimental results. In addition, a discussion of computational predictions of the characteristics of the signal received in the far zone when such an oscillator array excites a linear array of radiating elements is included.

**Index Terms**—Modulation, phase-locked oscillators, phased arrays, voltage-controlled oscillators.

## I. BACKGROUND

POGORZELSKI *et al.* [1] recently reported the design, fabrication, and test of a seven-element *S*-band coupled-oscillator-based phased-array antenna. The steady state of behavior of the aperture phase was shown to be linear and its slope could be controlled by the tuning of the end oscillators of the array. Thus, the end oscillator tuning ports were shown to be control ports for beam steering of the radiation from the array. In applications of such arrays to communications systems, it will be necessary to modulate the frequency or phase of the radiated beam with information to be transmitted. This will require an understanding of the dynamics of the phase distribution over the array. Such an understanding can be acquired by means of a linearized theory developed by Pogorzelski *et al.* [2], which shows that the dynamic behavior of the phase distribution is governed by a diffusion equation. Thus, the dynamic behavior of the aperture phase and its implications for modulation of the array can be obtained by solution of this equation.

In this paper, an experimental confirmation of the validity of the diffusion model is presented. This confirmation provides a firm basis upon which to build a description of the modulation properties of coupled-oscillator arrays [3].

## II. THEORETICAL PREDICTION

The continuum approach to the phase dynamics leads to a diffusion equation of the form

$$\frac{\partial^2 \phi}{\partial x^2} - \frac{1}{\Delta\omega_{\text{lock}}} \frac{\partial \phi}{\partial t} = -\frac{\omega_{\text{tune}} - \omega_{\text{ref}}}{\Delta\omega_{\text{lock}}} \quad (1)$$

Manuscript received August 21, 2000; revised January 30, 2001. This work was supported under a contract by the National Aeronautics and Space Administration.

The author is with the Jet Propulsion Laboratory, California Institute of Technology, Pasadena, CA 91109-8099 USA.

Publisher Item Identifier S 0018-9480(02)00025-X.

in which  $x$  is a continuous variable, which takes on integer values indexing the oscillators of the array,  $\omega_{\text{tune}}$  (which is a function of  $x$ ) is the distribution of free running frequencies of the oscillators,  $\Delta\omega_{\text{lock}}$  is the inter-oscillator locking range,  $\omega_{\text{ref}}$  is a reference frequency used in defining the phase, and  $\phi(x, t)$  is a continuous function of  $x$ , which takes a value equal to the phase of a given oscillator when its first argument  $x$  takes on an integer value indexing that oscillator. If one oscillator of the array is step detuned by an amount  $C$  measured in locking ranges, it can be shown that the dynamic solution of (1) for the phase  $\phi(x, t)$  is [2]

$$\begin{aligned} \phi(x, t) = & \frac{C\Delta\omega_{\text{lock}}t}{2a+1} + C \sum_{n=0}^{\infty} \frac{2 \cos(b\sqrt{\sigma_n}) \cos(x\sqrt{\sigma_n})}{(2a+1)\sigma_n} \\ & \times (1 - e^{-\sigma_n \Delta\omega_{\text{lock}}t}) \\ & + C \sum_{m=0}^{\infty} \frac{2 \sin(b\sqrt{\sigma_m}) \sin(x\sqrt{\sigma_m})}{(2a+1)\sigma_m} \\ & \times (1 - e^{-\sigma_m \Delta\omega_{\text{lock}}t}) \end{aligned} \quad (2)$$

where

$$\sigma_n = \left( \frac{2n\pi}{2a+1} \right)^2 \quad (3)$$

for  $n = 0, 1, 2, \dots$ ,

$$\sigma_m = \left( \frac{(2m+1)\pi}{2a+1} \right)^2 \quad (4)$$

for  $m = 0, 1, 2, \dots$ ,  $b$  is the value of  $x$  indexing the detuned oscillator, and  $2a+1$  is the number of oscillators in the array. In steady state, this solution becomes

$$\begin{aligned} \phi_{ss}(x) = & C \sum_{n=0}^{\infty} \frac{2 \cos(b\sqrt{\sigma_n}) \cos(x\sqrt{\sigma_n})}{(2a+1)\sigma_n} \\ & + C \sum_{m=0}^{\infty} \frac{2 \sin(b\sqrt{\sigma_m}) \sin(x\sqrt{\sigma_m})}{(2a+1)\sigma_m} \\ = & \frac{C}{2(2a+1)} \\ & \times \left[ x^2 + b^2 - (2a+1)|b-x| + \frac{1}{6}(2a+1)^2 \right]. \end{aligned} \quad (5)$$

Consider now an array of seven oscillators ( $a = 3$ ) and let the rightmost oscillator be detuned ( $b = 3$ ). The steady-state solution then becomes

$$\phi_{ss}(x) = \frac{C}{14} \left[ x^2 + 7x - \frac{23}{6} \right] \quad (6)$$

which is a parabola with zero slope at the left-hand edge of the array ( $x = -3.5$ ). If the phase of the center oscillator is taken to be the reference, the solution is shifted by an additive constant and the result becomes

$$\phi_{ss}(x) = \frac{C}{14} x[x + 7] \quad (7)$$

which, of course, still has zero slope at the left-hand edge of the array.

If the oscillator immediately to the right-hand side of the center one were detuned, i.e.,  $b = 1$ , the solution corresponding to (6) is

$$\phi_{ss}(x) = \frac{C}{14} \left[ x^2 + 9 - 7|1 - x| \right] \quad (8)$$

and if the center oscillator is taken to be the phase reference, the result corresponding to (7) is

$$\phi_{ss}(x) = \frac{C}{14} \left[ x^2 + 7 - 7|1 - x| \right] \quad (9)$$

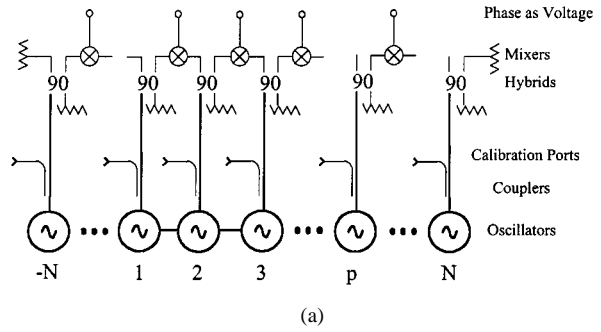
which has zero slope at both ends of the array.

### III. EXPERIMENT

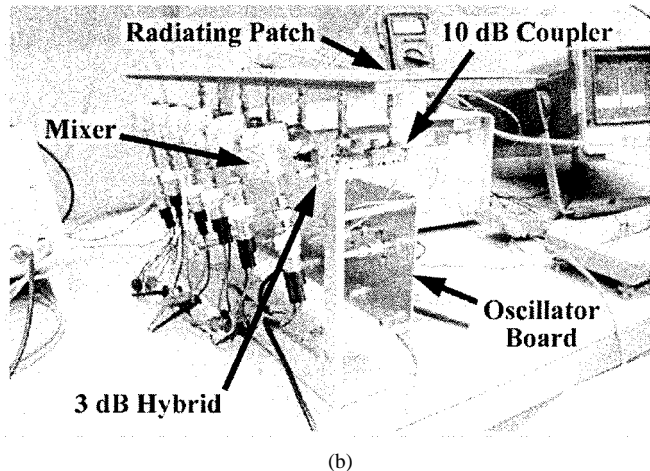
The seven-element array described in [1] was used to test the above theoretical predictions. The aperture phase was measured using a set of 3-dB hybrid couplers and mixers arranged to indicate the phase difference between adjacent oscillators, as shown in Fig. 1(a). The output voltages of the mixers were digitized and processed as channels 1–6 in a virtual instrument programmed in Labview. The physical array with the phase diagnostic system is shown in Fig. 1(b). (Here, the calibration ports of Fig. 1(a) were connected to radiating elements for range testing reported elsewhere [1].) The mixer output voltages were converted to phase using previously determined calibration constants as follows. The dc component of the output voltage of the mixer, i.e.,  $V_{dc}$ , is related to the phase difference between the outputs of the adjacent oscillators connected to it through the hybrids  $\Delta\phi$  by

$$V_{dc} + V_{offset} = S \sin(\Delta\phi - \phi_{offset}) \text{ or,} \\ \Delta\phi = \phi_{offset} + \sin^{-1} \left( \frac{V_{dc} + V_{offset}}{S} \right) \quad (10)$$

where  $S$  represents the sensitivity of the system to phase differences,  $V_{offset}$  is the output voltage when the argument of the sine function is zero, and  $\phi_{offset}$  accounts for the difference in electrical length of the RF and local-oscillator (LO) paths into the mixer. These three constants are determined during the calibration process in which a network analyzer is connected to pairs of adjacent calibration ports (see Fig. 1) to accurately measure the phase difference in oscillator outputs, and the constants are adjusted to make the virtual instrument register the correct phase difference. Taking the center oscillator as a reference, the phase



(a)



(b)

Fig. 1. (a) Aperture phase diagnostic system concept. (b) Implementation of the aperture phase diagnostic system.

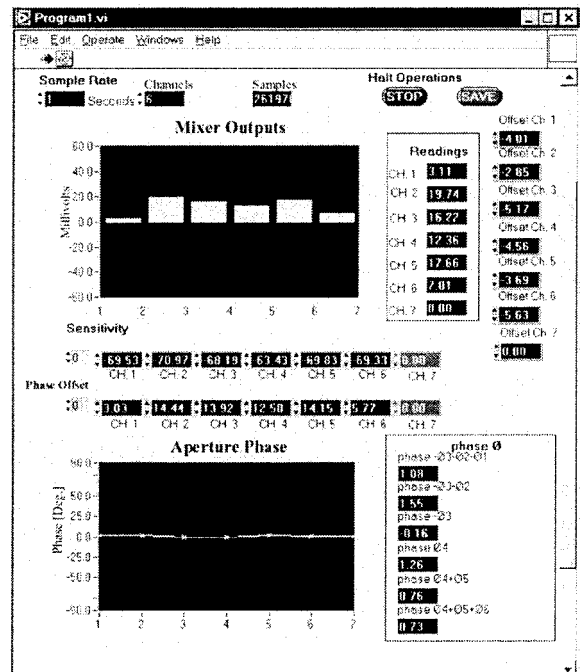


Fig. 2. Virtual instrument display—uniform aperture phase.

differences were integrated to determine the aperture phase distribution and the result was displayed graphically. Fig. 2 shows the virtual instrument display when the oscillators are tuned to produce a uniform phase distribution corresponding to a beam radiated normal to the radiating aperture. Note that the three

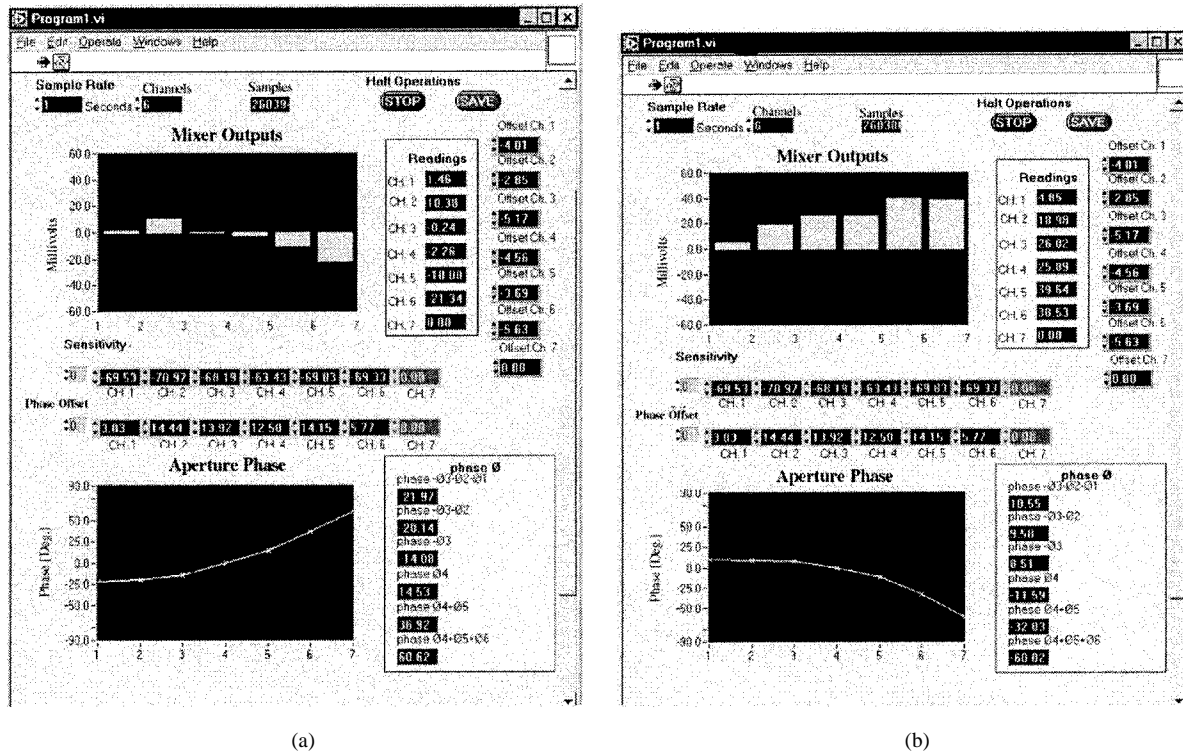


Fig. 3. (a) Steady-state phase distribution with the rightmost oscillator tuned upward. (b) Steady-state phase distribution with the rightmost oscillator tuned downward.

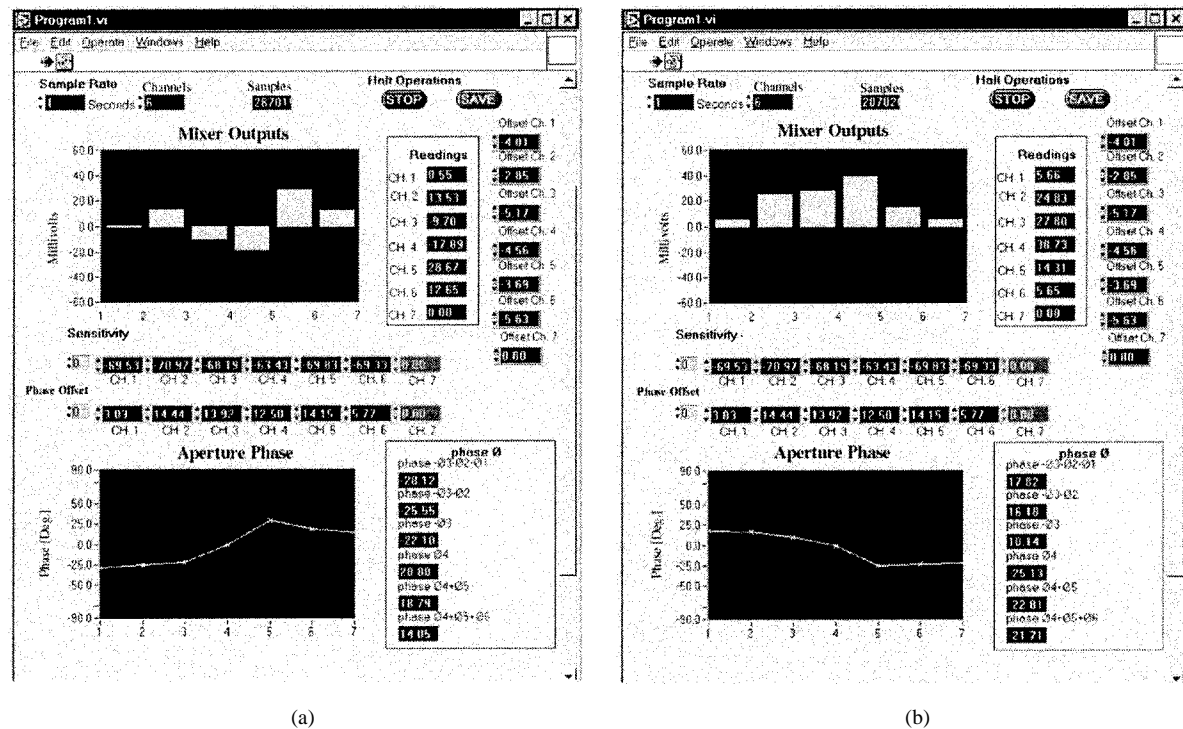


Fig. 4. (a) Steady-state phase distribution with the oscillator immediately to the right-hand side of the center oscillator tuned upward. (b) Steady-state phase distribution with the oscillator immediately to the right-hand side of the center oscillator tuned downward.

calibration constants for each mixer are shown numerically as voltage offsets associated with the top plot showing mixer outputs in millivolts, and as sensitivities and phase offsets shown above the bottom plot of the phase distribution. The abscissae of these graphs index the seven oscillators and are equal to  $x + 4$ ,

where  $x$  is the oscillator index used in the theoretical development. The column labeled ‘Readings’ displays the quantity  $V_{dc} + V_{offset}$ .

Tuning of these voltage-controlled oscillators is accomplished by application of bias voltage to a varactor in the

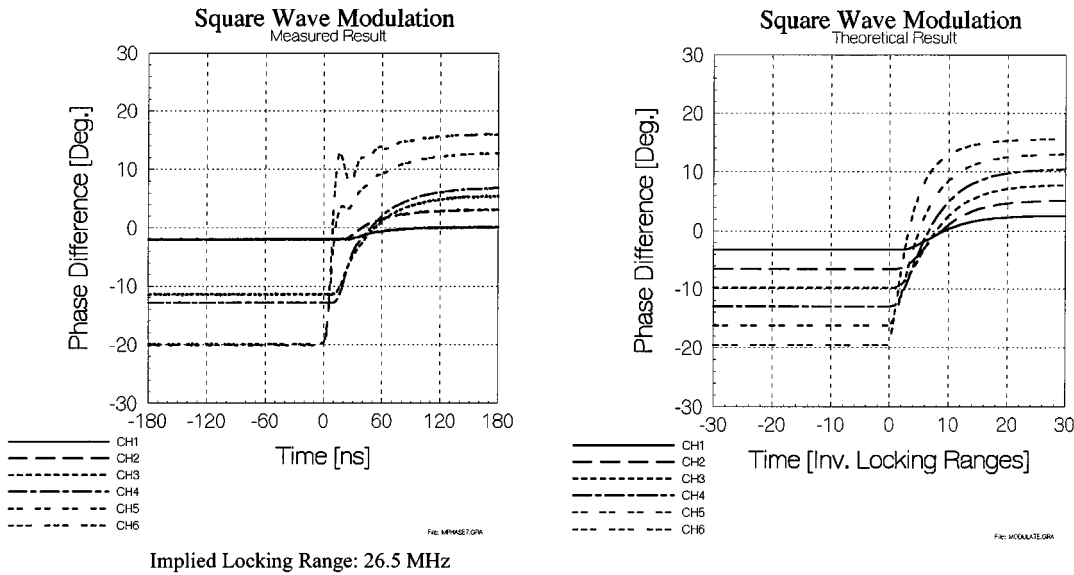


Fig. 5. Measured and theoretical transient response of the array with the rightmost oscillator modulated.

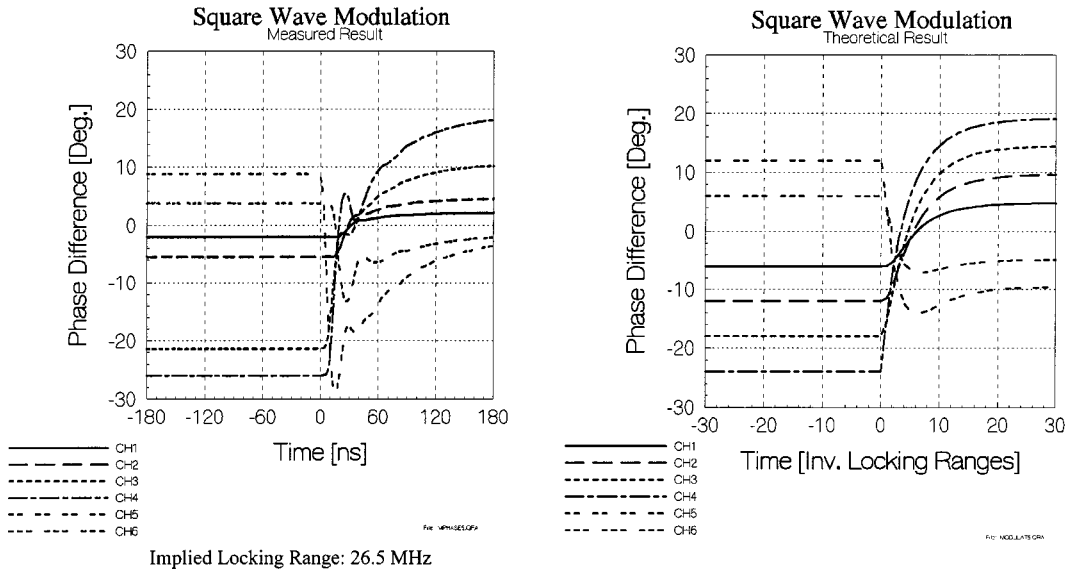


Fig. 6. Measured and theoretical transient response of the array with the oscillator immediately to the right-hand side of the center oscillator modulated.

resonant tank circuit of each oscillator. Fig. 3(a) shows the phase distribution that results if the rightmost oscillator is detuned upward in frequency such that its phase becomes  $60^\circ$ . Fig. 3(b) shows the corresponding result if it is tuned downward in frequency. These results confirm (7) with  $C$  approximately 0.5 locking ranges. If the oscillator immediately to the right-hand side of the center one is similarly detuned, results are obtained as shown in Fig. 4. This confirms (9) with  $C$  approximately 0.8 locking ranges.

To test the dynamic solution (2), a 1-kHz square wave was applied to the tuning port of the rightmost oscillator and the transient phase response was recorded using a Tektronix TDS-3054 four-channel oscilloscope and plotted. Using (2), the corresponding theoretical prediction was then computed. The value of  $C$  corresponding to the square wave applied was approximately 0.4. Graphs of the measured and computed results are shown in Fig. 5. The ordinates of these graphs are the

phase *differences* between adjacent oscillators as determined by measurement of the dc output voltages of the corresponding mixers. Thus, equal vertical spacing of the curves indicates a linear phase *gradient* and a quadratic phase *distribution* across the array. By comparing the time scale of the plots, the locking range was estimated to be 26.5 MHz, which is consistent with direct measurement. The “ringing” evident in the measured data was inherent in the square-wave generator that was employed. That is, the ringing is present in the driving function and is not intrinsic to the array behavior. Fig. 6 shows the corresponding data when the square-wave voltage ( $C \approx 0.6$ ) was applied to tune the oscillator immediately to the right-hand side of the center one. Here again, the theoretical predictions are confirmed by the measurements.

The theoretical predictions are based on the assumption that the amplitude of the oscillations and the tuning sensitivities are uniform throughout the array. In fact, this is not the case, and

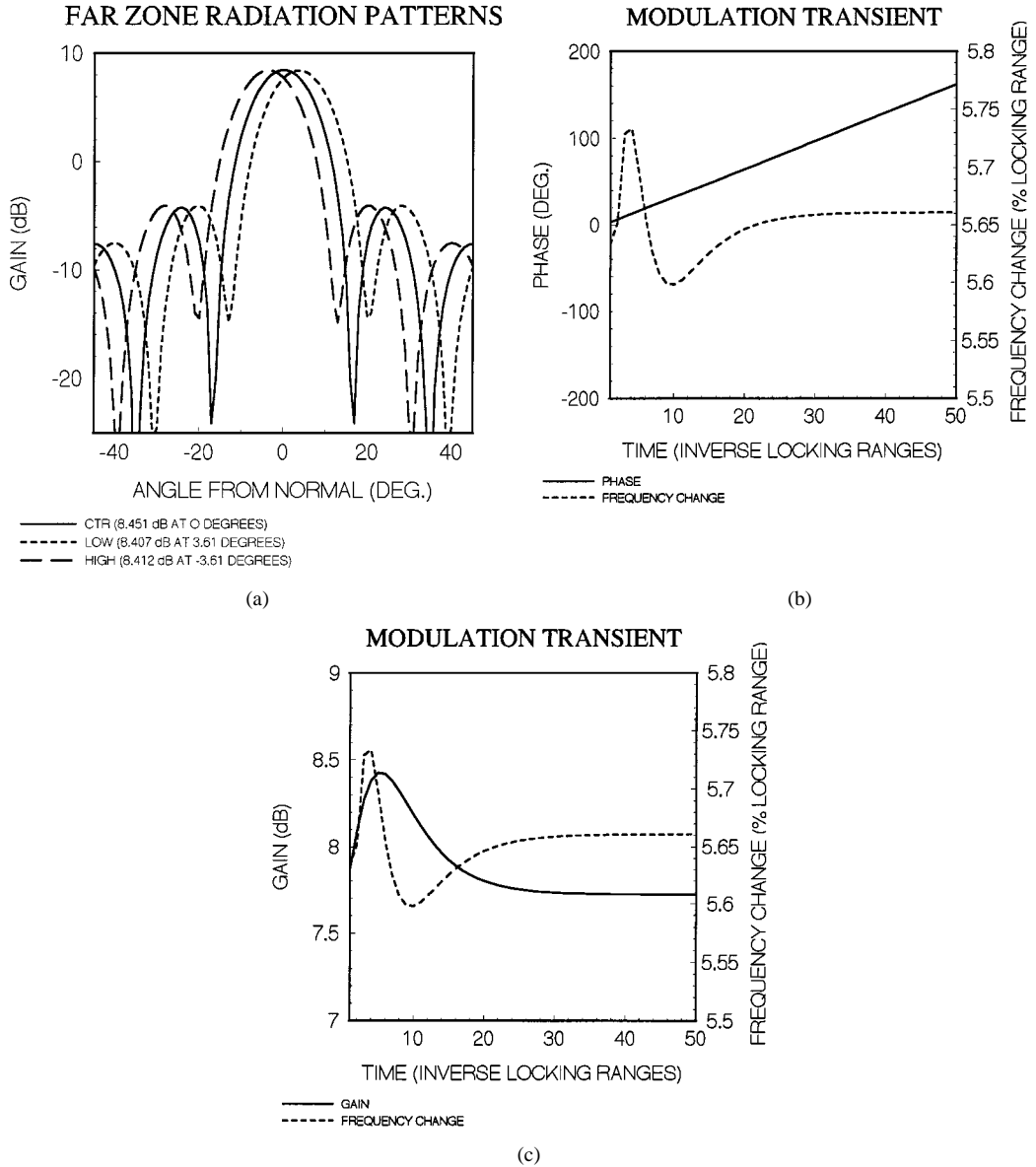


Fig. 7. (a) Radiation patterns with end oscillator modulated. (b) Phase and frequency transient with end oscillator modulated. (c) Amplitude and phase transient with end oscillator modulated.

this represents a source of discrepancy between the measured and predicted behaviors manifest in particular in the nonuniform spacing of the experimental curves. Nevertheless, the dynamic behavior of the phase closely resembles the theoretical results.

#### IV. IMPLICATIONS FOR MODULATED ARRAYS

The predictions of the linearized continuum model concerning both the static and dynamic behavior of coupled oscillator arrays have been confirmed by experiment. Moreover, it is clear that if frequency modulation is applied to a single oscillator of the array, the aperture phase distribution becomes parabolic, thus spoiling the beam. This is not a transient effect in that it remains true in steady state. Thus, in principle, no matter how slowly a single oscillator is modulated, the array will not radiate a pure frequency modulated beam. Rather, as

the oscillator tuning is switched from the high frequency to the low one, the beam will oscillate between two spoiled states of differing gain. This clearly shows that efficient radiation of a true frequency modulated beam can only be accomplished by frequency modulating every oscillator in the array simultaneously. Fortunately, this is not difficult because the distribution of the modulation signal is a baseband distribution, thus, not requiring an equal line length (corporate) feed network of any kind.

The degree of beam spoiling to be expected remains to be estimated. This can be computed using the same theoretical framework used to compute the transient responses that were compared with the above experimental results. We merely compute the far-zone pattern (amplitude and phase) radiated by a seven-element array of isotropic elements spaced one half-wavelength apart at the center frequency and excited by the oscillator array whose transient response was studied above. The frequency of

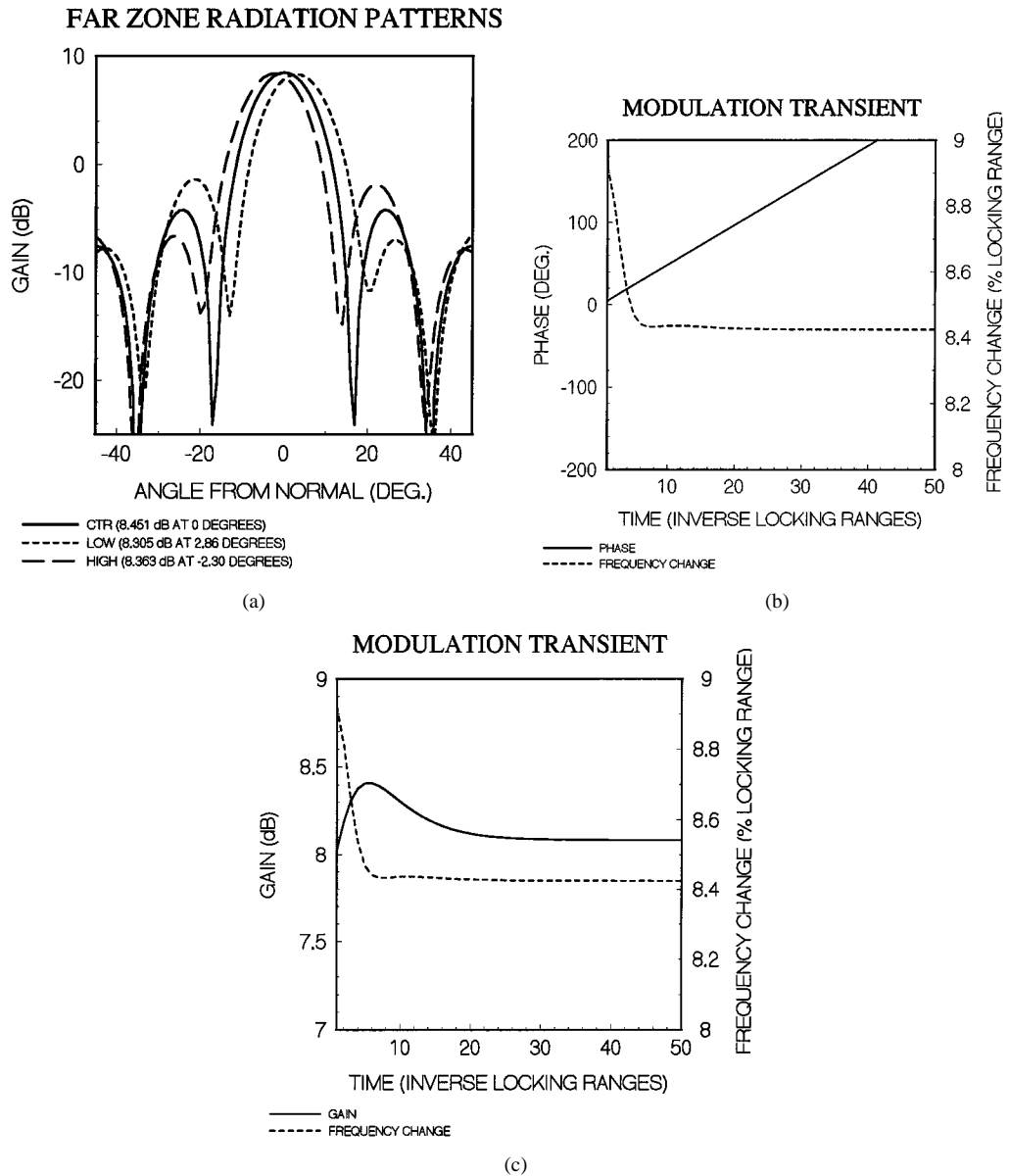


Fig. 8. (a) Radiation patterns with oscillator 1 modulated. (b) Phase and frequency transient with oscillator 1 modulated. (c) Amplitude and phase transient with oscillator 1 modulated.

the radiated signal may then be computed by numerical differentiation of the phase with respect to time. These calculations were performed for the two transient cases shown in Figs. 5 and 6 and the results are shown in Figs. 7 and 8, respectively.

Fig. 7(a) shows the radiation patterns when the end oscillator is tuned downward (LOW), upward (HIGH), and for the nominal tuning (CTR). Note that the quadratic phase aberrations for the LOW and HIGH cases reduce the peak gain by about 0.04 dB, which is a negligible amount. More importantly, however, these aberrations shift the angular position of the beam peak right and left by about  $3.6^\circ$ . Thus, the on axis gain, i.e., the gain perceived by a receiver on a line normal to the array, is decreased by 0.76 dB in the spoiled states relative to the uniform phase case. Even this may not be significant because, in any angle-based modulation scheme, one typically limits the amplitude such that small variations do not affect the received information. The actual channel capacity is governed by the rate at which the fre-

quency of the received signal can be changed. To study this aspect of the system, the transient phase and frequency of the received on axis signal were computed as shown in Fig. 7(b). The phase is linearly dependent on time because of the shift in ensemble frequency induced by the detuning of the end oscillator. As shown, the steady-state frequency is shifted by 5.66% of the locking range or about 1.5 MHz. This is one-seventh of the detuning of the end oscillator, i.e., the modulation index is reduced by a factor of the number of oscillators in the array. It should be remarked that this places a limit on the attainable modulation index in that the amount by which the end oscillator may be detuned is itself limited to one locking range by the  $90^\circ$  maximum phase difference between adjacent oscillators [2]. The transient in the frequency curve decays in about 25 inverse locking ranges or about a microsecond. Of course, during this transient, the aperture phase is evolving from one parabolic distribution to the other and passes through a condition of nearly

uniform phase. This is manifest in the gain transient shown in Fig. 7(c), where the gain peak reaches 8.425 dB, which is nearly the ideal 8.451 dB obtained with a uniform aperture phase. The results corresponding to the case of Fig. 6, where oscillator 1 is modulated, are shown in Fig. 8. Here, the beam peaks are reduced by only 0.1–0.14 dB, the on axis gain is reduced only 0.68 dB in the spoiled states, and the maximum detuning of the oscillator is limited to two locking ranges. If, however, the center oscillator were modulated, the beam peak would, of course, remain on axis, and similar computations show that the gain reduction due to beam spoiling would be only about 0.06 dB, the sidelobes of the radiation pattern would be increased by about 0.5 dB, and the maximum permitted detuning remains two locking ranges.

From the above analysis, one may conclude that, while modulation of one oscillator yields performance that is inferior to that obtained by modulation of all the oscillators, it nevertheless offers a simple alternative that may provide acceptable results.

#### ACKNOWLEDGMENT

The research described in this paper was performed by the Telecommunications Science and Engineering Division, Jet Propulsion Laboratory (JPL), California Institute of Technology, Pasadena. The help of M. S. Zawadzki, JPL, and J. S. Acorn, JPL, in construction and calibration of the diagnostic system, is appreciatively acknowledged.

#### REFERENCES

- [1] R. J. Pogorzelski, R. P. Scaramastra, J. Huang, R. J. Beckon, S. M. Petree, and C. Chavez, "A seven element *S*-band coupled oscillator controlled agile beam phased array," *IEEE Trans. Microwave Theory Tech.*, vol. 48, pp. 1375–1384, Aug. 2000.
- [2] R. J. Pogorzelski, P. F. Maccarini, and R. A. York, "A continuum model of the dynamics of coupled oscillator arrays for phase shifterless beam-scanning," *IEEE Trans. Microwave Theory Tech.*, vol. 47, pp. 463–470, Apr. 1999.
- [3] R. J. Pogorzelski, J. S. Acorn, and M. S. Zawadzki, "On the modulation of coupled oscillator arrays in phased array beam control," in *Nat. Radio Sci. Meeting Dig.*, Boulder, CO, Jan. 2000, p. 67.



**Ronald J. Pogorzelski** (S'61–M'69–SM'82–F'95) received the B.S.E.E. and M.S.E.E. degrees from Wayne State University, Detroit, MI, in 1964 and 1965, respectively, and the Ph.D. degree in electrical engineering and physics from the California Institute of Technology, Pasadena, in 1970.

From 1969 to 1973, he was an Assistant Professor of engineering at the University of California at Los Angeles, where his research dealt with relativistic solution of Maxwell's equations. From 1973 to 1977, he was an Associate Professor of electrical engineering at the University of Mississippi, where his research interests encompassed analytical and numerical aspects of electromagnetic radiation and scattering. In 1977, he joined TRW as a Senior Staff Engineer and remained there until 1990, where he served as the Subproject Manager in the Communications and Antenna Laboratory, and as the Department Manager and Manager of the Senior Analytical Staff in the Electromagnetic Applications Center. From 1981 to 1990, he was also on the faculty of the University of Southern California, initially as a Part-Time Instructor and then as an Adjunct Full Professor. In 1990, he joined the General Research Corporation, Santa Barbara, CA, as the Director of the Engineering Research Group. Since 1993, he has been with the Jet Propulsion Laboratory, California Institute of Technology, where he is currently a Senior Research Scientist and the Supervisor of the Spacecraft Antenna Research Group. He is also a Lecturer in electrical engineering at the California Institute of Technology. He has authored or co-authored over 100 technical publications and presentations. He is listed in *American Men and Women of Science*.

Dr. Pogorzelski is a member of Tau Beta Pi, Eta Kappa Nu, and Sigma Xi. He has been elected a full member of U.S. National Committee (USNC)/International Scientific Radio Union (URSI) Commissions A and B and is the current vice-chair of U.S. Commission B. Over the years, he has served on a number of symposium committees and chaired a number of symposium sessions. He was vice chairman of the Steering Committee for the 1981 IEEE Antennas and Propagation Society (IEEE AP-S) Symposium, Los Angeles, CA, and the Technical Program chair for the corresponding symposium held in Newport Beach, CA, in 1995. From 1980 to 1986, he was an associate editor of the *IEEE TRANSACTIONS ON ANTENNAS AND PROPAGATION* and, from 1986 to 1989, he served as its editor-in-chief. From 1989 to 1990, he served as secretary/treasurer of the Los Angeles Chapter of the IEEE AP-S, was a member of the IEEE AP-S Administrative Committee from 1989 to 2000, served as vice president of the IEEE AP-S in 1992, and was the IEEE AP-S 1993 president. From 1989 to 1992, he was a member of the IEEE AP-S IEEE Press Liaison Committee. He has also represented the IEEE Division IV on the Technical Activities Board Publication Products Council, Periodicals Council, and New Technology Directions Committee. In 1995, he also served as a member of a Blue Ribbon Panel, which evaluated the Army's Team Antenna Program in helicopter antennas. He has recently completed a ten-year term as a program evaluator for the Accreditation Board for Engineering and Technology. In 1984, he was appointed an Academy Research Council Representative to the XXIst General Assembly of the URSI, Florence, Italy, and in 1999, to the XXVIth General Assembly of the URSI, Toronto, ON, Canada. He has been a member of the Technical Activities Committee of U. S. Commission B and has also served on its Membership Committee since 1988, where he currently serving as its chair. He was appointed to a two-year term as member at large of the U.S. National Committee of the URSI in 1996, and again in 1999. In 1980, he was the recipient of the R. W. P. King Award of the IEEE AP-S for a paper on propagation in underground tunnels. He was also the recipient of the IEEE Third Millennium Medal.